Critical behavior of an autocatalytic reaction model

T. Aukrust, D. A. Browne,* and I. Webman
IBM Bergen Scientific Centre, Thormøhlensgate 55, N-5008 Bergen, Norway
(Received 23 October 1989)

Irreversible many-particle dynamical systems are relevant to a variety of phenomena in physics, chemistry, and biology. We present a study of an irreversible kinetic reaction model for a one-component autocatalytic reaction $A + A \rightarrow A_2$. In this model, if an atom adsorbing on a lattice site has any neighbors, it reacts with one of them with a probability $1-p$, and the two atoms leave the lattice; otherwise the atom occupies the site. As p is varied, this model undergoes a second-order kinetic phase transition from a chemically reactive state with a partial occupation of the lattice to a completely covered state that corresponds to the "poisoning" phenomenon seen on catalysts. The transition is studied both analytically through various mean-field approximations and numerically in one, two, and three dimensions. Finite-size-scaling analysis of the critical behavior is used to find the static and dynamic critical exponents. These exponents are found to be consistent with the critical exponents in the Reggeon-field-theory directed-percolation universality class.

I. INTRODUCTION

Irreversible dynamical many-particle systems are relevant to a broad scope of phenomena in physics, chemistry, and biology. Some of these systems are known to possess kinetic phase transitions where macroscopic properties of the steady state behave in a singular fashion as the rates for various microscopic processes are varied. But, in contrast to critical phenomena in equilibrium systems where a successful theory has been established, our understanding of phase transitions in nonequilibrium systems is still poor. Thus more insight, both in the behavior and in the description of dynamical phase transitions, is desirable.

Recently, Ziff, Gulari, and Barshad[1] (ZGB) introduced a simple kinetic reaction model to describe the chemical reaction $CO+O \rightarrow CO_2$ on a catalytic surface. In the model, the coverages of adsorbed molecules were found to undergo both first-order and second-order kinetic phases transitions. The surface of the catalyst is represented by a square lattice, and it is assumed that CO molecules and O atoms both occupy single lattice sites. CO and O_2 molecules are added randomly to the lattice, according to the relative ratio of their molecular concentration in the gas above the surface, Y_{CO} and $1-Y_{CO}$, respectively. It is further assumed that the adsorption of an oxygen molecule requires two adjacent empty sites. If oxygen atoms and CO molecules occupy nearest-neighbor lattice sites, CO-O pairs are randomly selected, producing CO_2 molecules which escape from the surface.

Ziff, Gulari, and Barshad[1] found that, for Y_{CO} below a certain value Y_1, the lattice is completely covered by oxygen atoms in the steady state and the reaction ceases. Above a second value, Y_2, the lattice is filled with CO. Only in the range $Y_1 < Y_{CO} < Y_2$ does the system show a mixed phase which is catalytically active. The transition from the mixed phase to the oxygen-covered phase was found to be second order (continuous), while the transition from the mixed phase to the CO-covered phase was was found to be discontinuous. These transitions correspond to poisoning transitions frequently seen in real catalysts.

In simulations of the ZBG model, Meakin and Scalapino[2] found that $1-n_O$ and n_{CO}, where n_O and n_{CO} are the fraction of oxygen and CO on the surface, respectively, behaved near the second-order transition as $(Y-Y_1)^{\beta}$, where β for the two quantities was found to be approximately $\beta_O \sim 0.69$. However, they stated that the uncertainty in the exponents suggested that the two values of β should be the same. Based on these numerical results it is not clear to which universality class the ZGB model belongs. Dickman and Burschka[3] introduced a simplified model to mimic the second-order phase transition in the ZGB model. From Monte Carlo simulations and field-theory calculations, they found that their model belonged to the Reggeon-field-theory[4] (RFT) universality class, to which directed percolation[5] (DP) also belongs[6]. Recently, Grinstein, Lai, and Browne[7] argued on the basis of a simple renormalization-group approach coupled with a finite-size scaling analysis of numerical estimates of the static critical exponents that the original ZGB model should be in the RFT universality class. Thus the exponent of Meakin and Scalapino should be compared with the known[8] exponent $\beta \sim 0.58$ for the RFT in two dimensions (2D). However, more accurate results and new numerical approaches to produce accurate values for both the static and dynamic critical exponents are clearly needed.

The ZGB model is relatively complex, primarily due to the presence of two reacting species and the requirement that there be two vacant nearest-neighbor sites for the addition of the oxygen molecules. In an effort to understand the phase transitions in the ZGB model and related models for nonequilibrium systems, we have made a careful examination of a simpler one-component autocatalytic reaction model introduced by Browne and Kleban[9] (BK).

In this latter model atoms of a single species can adsorb on empty sites of a lattice. The reaction rules in this model contain a single parameter p which controls the relative probability of an atom to simply stick on an empty site versus immediately reacting with an atom occupying a neighboring site. A phase transition from a chemically active partially covered state to a fully covered inactive state occurs as p is increased to a certain critical value.

In Sec. II the BK model is described. In Sec. III we present mean-field results and numerical results for the kinetic phase transition. In Sec. IV we show that in spite of the strong tendency of the model to cover in the critical region, average values can be obtained by finite-size scaling. In this section results for both the steady-state behavior and the dynamical behavior are presented, along with estimates of the critical exponents in one, two, and three dimensions. In Sec. V we give a short discussion and conclusions. A preliminary report of our results for the one- and two-dimensional versions of these models has appeared elsewhere.[10]

II. MODEL

The BK model[9] corresponds to a two-state asynchronous cellular automaton.[11] Each lattice site can be either in a state A (occupied by an atom) or in state V (vacant). At a given time step a site is chosen at random. The rules for the evolution of the system then take into account the current state of the chosen site and the state of its nearest neighbors in the following fashion. If the chosen site is in the state A, it is unchanged. If the site is vacant (V), then the update depends on the number of nearest-neighbor sites that are occupied. If none are occupied, the chosen site is changed to A. If one or more of the neighboring sites are A, then with probability p the chosen site is converted to A and the neighbors are unchanged. Otherwise, one of the occupied neighbors is chosen randomly and vacated, with the central site remaining V.

This procedure corresponds to a flux of atoms impinging on a surface at random. A reaction $A+A\rightarrow A_2$ may occur where A_2 escapes the surface. The atoms arrive with some energy. Within a certain period of time from the instant of arrival the energy can prompt a reaction with a neighbor, or else dissipate into the lattice, in which case the atoms adsorb on the surface. The choice of an asynchronous cellular automaton is the most natural in this physical situation in which atoms land on surface sites in a stochastic manner.

These rules imply that a fully covered surface will always remain covered. So, for any value of p, a fully covered state is stable. In fact, for any finite system a consideration of these rules[9] leads to the conclusion that the fully covered state is the unique steady state, so the reactive state is only metastable in a finite system.

III. KINETIC PHASE TRANSITION

A. Mean-field results

We start this section by discussing a simple mean-field approximation. The site mean-field (SMF) approximation[12] is obtained by neglecting all correlations between the states of sites in the neighborhood of an updated single site. This assumption leads to the following equation for the rate of change of the volume fraction of vacancies X_0:

$$\frac{dX_0(t)}{dt}=-X_0(t)X_0(t)^n-(2p-1)X_0(t)[1-X_0(t)^n]\ , \tag{1}$$

where n is the number of neighbor sites on the lattice. This mean-field approximation is similar to the equations used in chemical kinetics approaches to these kinds of reactions. The approximation should become exact if strong mixing occurs, for example by including rapid surface diffusion in the model.[13] However we expect only qualitative agreement with the numerical work in the present case. For p less than the critical $p_c=\frac{1}{2}$ in SMF, Eq. (1) has the solution

$$X_0(t)=X_0(\infty)/[1+X_0(\infty)^n\tilde{X}e^{-t/\tau}]^{1/n}\ , \tag{2}$$

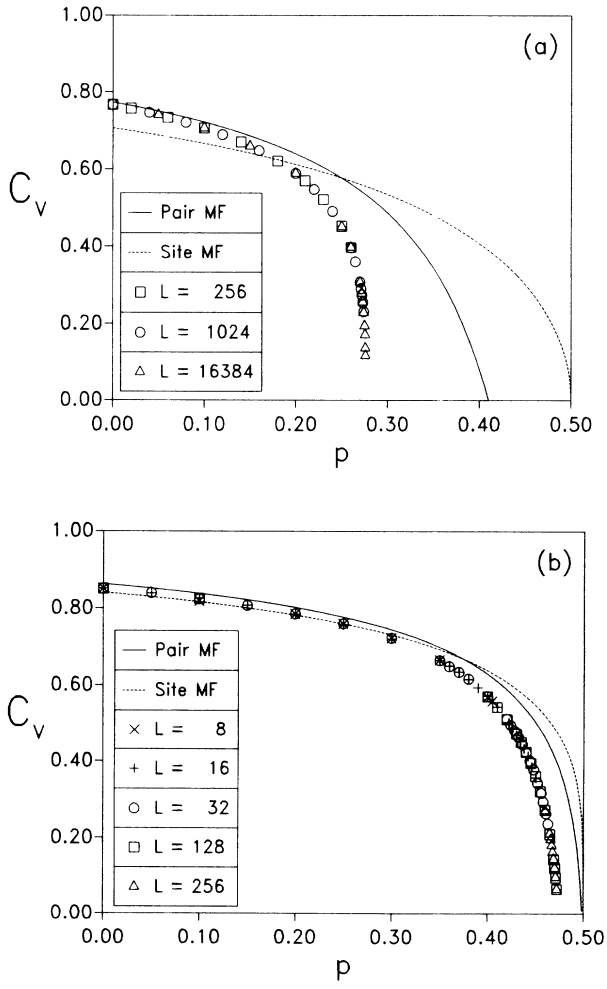

FIG. 1. Fraction of vacancies as a function of p for (a) the one-dimensional and (b) the two-dimensional models. The symbols show numerical results for various system sizes L. The dotted and the solid lines show the results from site mean field and pair mean field, respectively.

where

$$X_0(\infty)=\left[\frac{p_c-p}{1-p}\right]^{1/n}, \tag{3}$$

$$\tau=[2n(p_c-p)]^{-1}, \tag{4}$$

and $\tilde{X}$ is given by the initial condition. With the assumption that $X_0(\infty)\sim(p_c-p)^{\beta}$, the site mean field gives $\beta=1/n$, which depends on the number of nearest neighbors. Equation (4) yields a characteristic mean-field slowing down: $\tau\sim(p_c-p)^{-1}$.

In the pair mean-field approximation we have followed an approach similar to the one used by Dickman,[12] based on tracing the rate of change of all states of nearest-neighbor pairs of sites embedded in a medium without spatial correlations. The pair mean-field approximation gives $p_c=0.410$ in one dimension (1D) and $p_c=0.498$ in 2D with $\beta=1$ in both 1D and 2D.[10] In Figs. 1(a) and 1(b) we show the results for the 1D and the 2D versions of the model, respectively. The solid and the dotted lines in Figs. 1(a) and 1(b) represent the vacancy fraction obtained from a site mean field and a pair mean-field approximation, respectively. The mean-field approximation indicates that the covering transitions is continuous.

B. Numerical results for the vacancy fraction

The numerical simulations were carried out using the following procedure: A site is picked at random and updated according to the rules described above. One time unit or one Monte Carlo step (MCS) in the simulation corresponds to a number of updates equal to the number of sites in the lattice, i.e., in one MCS each site is visited once on the average. The simulation starts with an empty lattice. The time it takes the system to reach a stationary state depends on the lattice size L, and on the value of p. For $p=0$ the relaxation time is of the order one time unit, while close to p_c it is of order 10^4 time units for $L=128$ in the 2D case. A typical run close to p_c consists of 10^5 to 10^6 time units and the data are sampled from every 5 to every 100 time intervals.

The vacancy fraction exhibits fluctuations around the mean. Close to p_c these fluctuations are large and lead the system to the stable covered state. The characteristic time for this to happen depends upon $|p-p_c|$ and L. Near p_c large covered regions appear and covering is likely when the size of these regions becomes of order of the system size.

The vacancy fraction C_V, as a function of p is shown in Figs. 1(a) and 1(b) for the 1D and the 2D versions of the model, respectively. For each L, the data are shown only up to a value $p'<p_c$ where the system will cover within a reasonable run time. Assuming that C_V behaves as

$$C_V\sim|p_c-p|^{\beta}, \tag{5}$$

we have plotted $\log_{10}C_V$ versus $\log_{10}(p_c-p)$ and find $p_c=0.2762(5)$ and $\beta=0.28(2)$ for the 1D case, $p_c=0.4730(5)$ with $\beta=0.56(5)$ for the 2D case. The uncertainties in the last digits are shown in parentheses.

IV. FINITE-SIZE SCALING

From the nature of the model it is clear that close to and above p_c a finite system will become covered reasonably quickly. In Fig. 2 we show the time dependence of the fraction of vacancies C_V at $p=0.4730$ for a two-dimensional system of size 16×16. After a short transient, C_V reaches a reasonably steady value with large fluctuations characteristic for a system near a critical point. After the system has reached this quasiequilibrium state it will eventually become covered. The system shown in Fig. 2 remained uncovered for an unusually long time. Typically, system of size 16×16 will cover sooner for $p=0.473$ but we observed that the time required to cover varies wildly from one sample to the next. In Fig. 3 we show $\delta_s(t,L)=\langle C_V(t,L,s)\rangle_s$ versus time t for the one-dimensional version of the model for $p=0.2762$. Here δ_s is the average over the samples which have survived up to the time where the average is done. For each L we have started with 1000 samples s from the empty state. As in Fig. 2, Fig. 3 shows that, when a system is started from the empty state, it relaxes until an equilibrium state is reached where δ_s has a well-defined average value. After this state is reached covering takes place. This shows that, in spite of the strong tendency to cover, it is possible to obtain average values for $C_V(p,L)$ as a function of p and L in the critical region. Also it should be noted that both the characteristic time to reach the quasiequilibrium state and the average value for δ_s in this state depend on the system size L, as a result of finite-size effects.

As in a regular second-order phase transition we assume that the dynamical transition in our system features a length scale which diverges at criticality as $\xi\sim|p_c-p|^{-\nu_\perp}$ where $\nu_\perp$ is the correlation length exponent in the space direction. We chose to find $\nu_\perp$, and other critical exponents, by analyzing the finite-size scaling of both static and dynamic quantities, i.e., $C_V(p,L)$ and a characteristic time for the system.

For example, we assume the following scaling form for

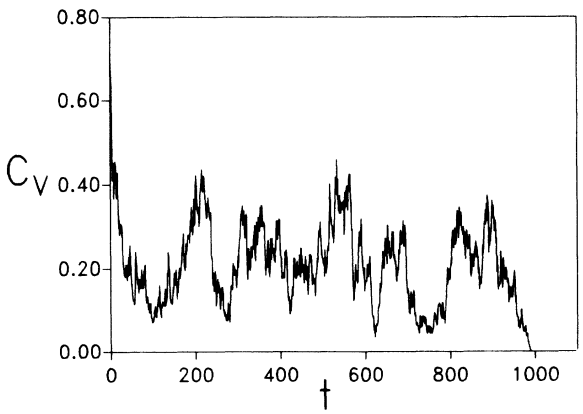

FIG. 2. The fraction of vacancies $C_V(t)$ as a function of time t for a two-dimensional system of size 16×16 at $p=0.4730$.

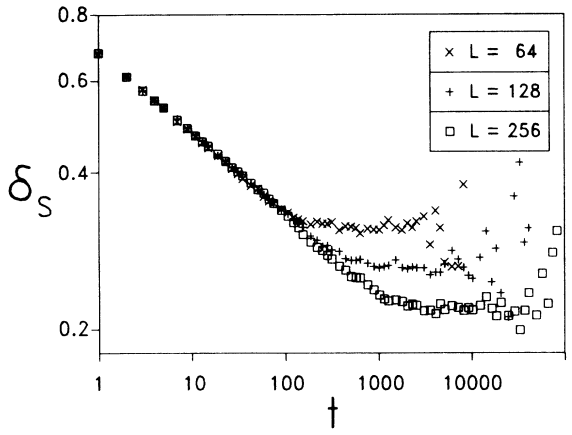

FIG. 3. $\delta_S(L,t)$ vs t for various system sizes L for the 1D version of the model, for $p=0.2762$ on a log-log scale.

the fraction of vacancies $C_V(p,L)$ in the critical region:

$$C_V(p,L)\sim L^{-\beta/\nu_\perp} f((p-p_c)L^{1/\nu_\perp}) , \tag{6}$$

so that at p_c

$$C_V(p_c,L)\sim L^{-\beta/\nu_\perp} , \tag{7}$$

and

$$f(x)\sim x^{\beta} \text{ for } x\to\infty , \tag{8}$$

such that Eq. (5) is recovered when $L\to\infty$ in the critical region.

One can also obtain the susceptibility χ normalized per lattice site, as

$$\chi = L^d(\langle C_V^2\rangle - \langle C_V\rangle^2) . \tag{9}$$

If $\chi\sim|p-p|^{-\gamma}$, one can also assume a finite-size scaling form for χ as

$$\chi(p,L)\sim L^{\gamma/\nu_\perp} g((p-p_c)L^{1/\nu_\perp}) , \tag{10}$$

such that at p_c

$$\chi(p_c,L)\sim L^{\gamma/\nu_\perp} . \tag{11}$$

As a characteristic time for our system we have chosen the time for a finite system to cover, for p above and in the vicinity of p_c. In order to measure this time, we start with an empty lattice and calculate for each sample s the fraction of vacancies $C_V(p,L,t,s)$ as a function of time t until the covered state is reached. We then calculate for each sample the moment τ_s,

$$\tau_s(p,L,s)=\sum_t tC_V(p,L,t,s)\Big/\sum_t C_V(p,L,t,s) . \tag{12}$$

We can see that τ_s is a measure of a characteristic time for the particular sample to cover by taking the example of a pure exponential relaxation for $C_V(t)$, where if $C_V(t)\sim\exp(-t/\alpha)$, then $\tau_s\sim\alpha$. In general, τ_s will depend on the system size L, the probability p, and the particular sample s.

For p much greater than p_c the sample quickly covers and τ_s is small. For p less than p_c, C_V will approach a finite average value. However, for a finite system this state is metastable and close to p_c fluctuations will eventually cause the system to cover. In this case one expects τ_s to increase much faster than a power law in L. In the thermodynamic limit ($L\to\infty$) we assume that as p_c is approached from above, $\tau=\langle\tau_s\rangle_s$, diverges as

$$\tau\sim(p-p_c)^{-\nu_\parallel} , \tag{13}$$

where $\nu_\parallel$ is the correlation exponent in the time direction. As for a second-order phase transition we assume that τ has a finite-size scaling form

$$\tau(p,L)\sim L^z h((p-p_c)L^{1/\nu_\perp}) , \tag{14}$$

where $z=\nu_\parallel/\nu_\perp$ is the usual dynamical exponent. At p_c we thus have

$$\tau(p_c,L)\sim L^z . \tag{15}$$

In their study of dynamical phase transitions, Neumann and Derrida[14] assumed a scaling form similar to Eq. (13) for the relaxation time for two different configurations submitted to the same thermal noise to become the same.

A. Scaling results for the static behavior

In order to do finite-size scaling for C_V, a number, typically 100 or so, of independent Monte Carlo runs were carried out for each p and L. Data from the quasiequilibrium uncovered state in the independent runs were then sampled. Each run began with an empty lattice and the simulation was run until the quasi-steady-state situation was reached. After that, sampling for averaging was done every 5–20 MCS until covering occurred. The mean value of C_V and fluctuations of C_V could then be found for each sample, and from the whole ensemble of Monte Carlo runs.

In Figs. 4(a)–4(c), we show $C_V(p,L)$ as a function of L in a log-log plot for the 1D, the 2D, and the 3D versions of the model, respectively. From Eq. (7), the data should fall on a straight line with slope $-\beta/\nu_\perp$ for $p=p_c$. Thus, the data give for the 1D case [Fig. 4(a)] $p_c=0.2762(3)$ and $\beta/\nu_\perp=0.254(10)$. For the 2D case we find [Fig. 4(b)] $p_c=0.4731(3)$ and $\beta/\nu_\perp=0.74(5)$. And Fig. 4(c) yields for the 3D case $p_c=0.4985(3)$ and $\beta/\nu_\perp=1.31(10)$. These estimates for p_c are consistent with the previous values. However, for the 3D case we have only gone up to $L=32$, and we suspect that there might be large corrections to scaling which will modify our results.

In Figs. 5(a)–5(c) we have plotted $C_V L^{\beta/\nu_\perp}$ versus $x=(1-p/p_c)L^{1/\nu_\perp}$ in a log-log plot for the data from the 1D, and 2D, and the 3D models, respectively. From Eqs. (6) and (8) it follows that for $|p-p_c|\ll 1$, the data in Fig. 5 should approach a constant, while for large arguments, $x\gg 1$, the data should fall on a line with slope β. For 1D [Fig. 5(a)] we find that with the choices $\beta=0.28(2)$ and $\nu_\perp=1.10(5)$ the data for the various system sizes superimpose. The solid line has a slope of 0.28, as should be

the asymptotic behavior for $C_V L^{\beta/\nu_\perp}$ as $L \to \infty$. In the same way, in 2D [Fig. 5(b)], we find good scaling with $\beta = 0.56(2)$ and $\nu_\perp = 0.75(5)$. For the 3D case we find scaling for $\beta = 0.79(7)$ and $\nu_\perp = 0.60(7)$ [Fig. 5(c)].

In Fig. 6 we show χ as a function of L for $p = 0.2762$ for the 1D case, and for $p = 0.4731$ for the 2D case. According to Eq. (11) the data at p_c should fall on a straight line with the slope $\gamma/\nu_\perp$. The data for 1D fall on a line with slope 0.51. With $\nu_\perp \sim 1.10$ that gives $\gamma \sim 0.56$. For the 2D case the data fall on a line with slope 0.50, which,

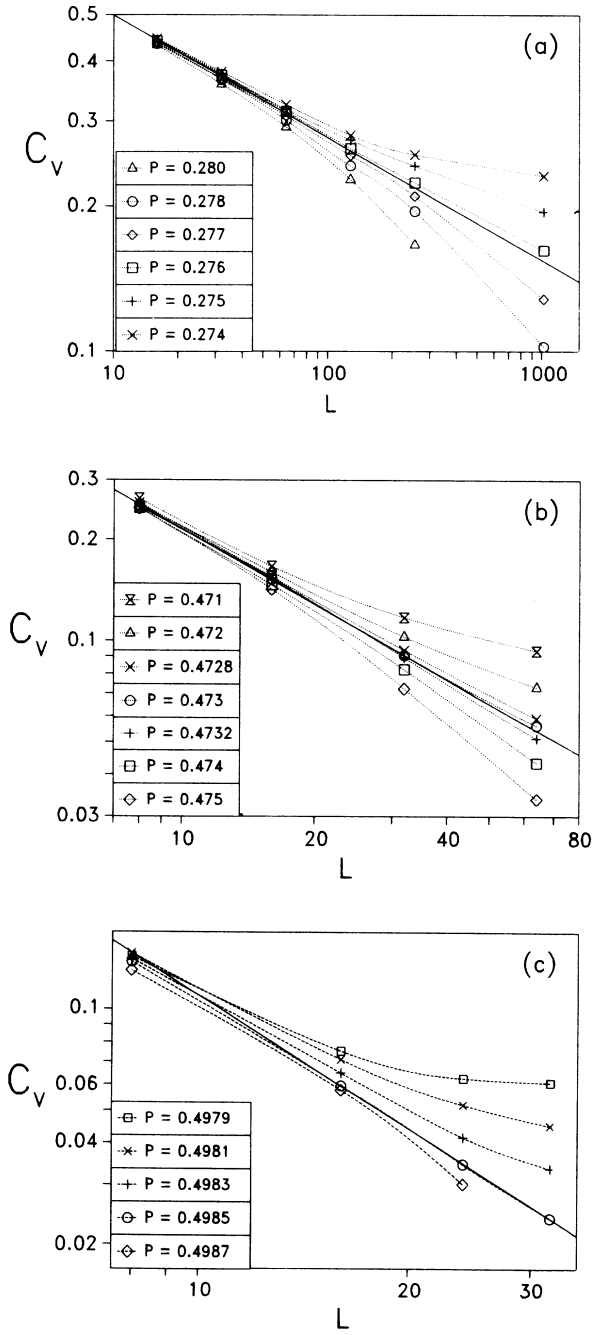

FIG. 4. $C_V(p,L)$ vs L for various values of p for (a) one, (b) two, and (c) three dimensions on a log-log scale. The slope of the straight line that goes through the data gives an estimate of $-\beta/\nu_\perp$. The slope is -0.254 for 1D (a), -0.741 for 2D (b), and -1.31 for 3D (c).

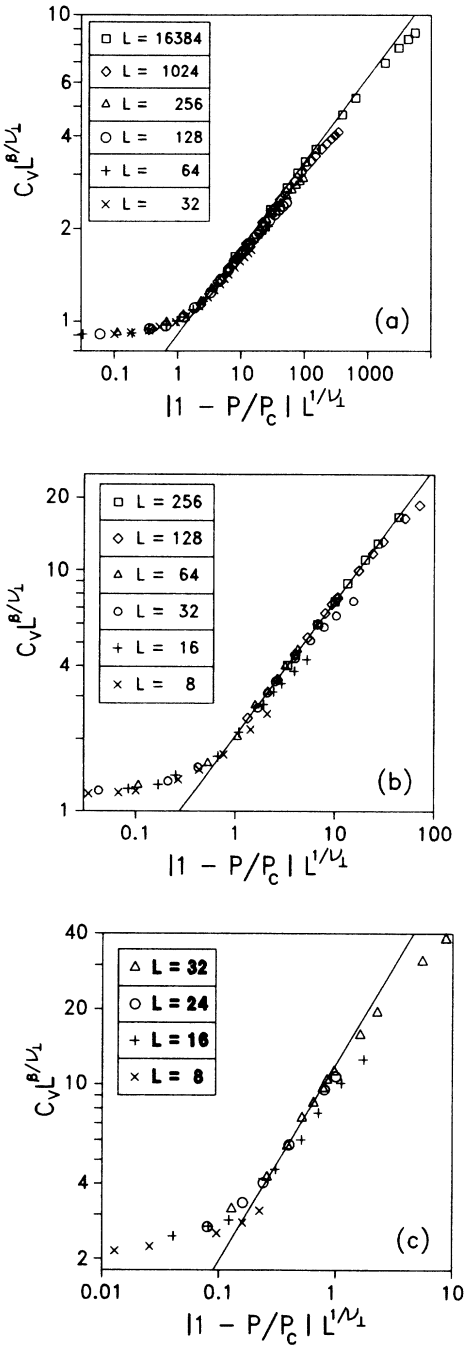

FIG. 5. Finite-size scaling of $C_V(p,L)$. $C_V L^{\beta/\nu_\perp}$ vs $x = (1 - p/p_c) L^{1/\nu_\perp}$ is shown in a log-log plot for (a) 1D, (b) 2D, and (c) 3D. In (a) $\beta = 0.28$ with $\nu_\perp = 1.10$ and $p_c = 0.2762$. In (b) $\beta = 0.557$ with $\nu_\perp = 0.752$ and $p = 0.4730$. In (c) $\beta = 0.79$ with $\nu_\perp = 0.60$ and $p = 0.4985$. The slopes of the solid lines in (a), (b), and (c), are 0.28, 0.557, and 0.79, respectively, which should be equal to β and the asymptotic behavior of $C_V L^{\beta/\nu_\perp}$.

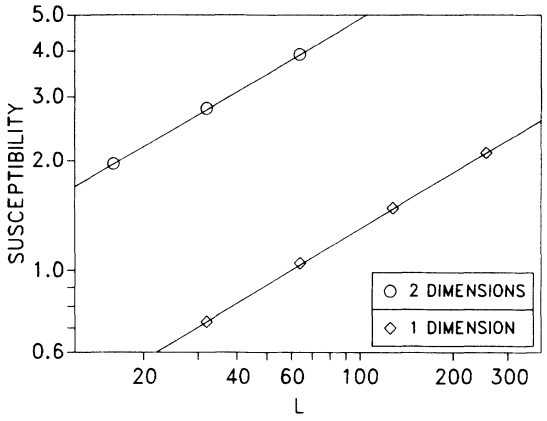

FIG. 6. The susceptibility χ for $\Diamond$, $p=0.2762$ in 1D, and $\circ$, $p=0.4730$ in 2D. The solid lines through the data in 1D and 2D have slopes of 0.51 and 0.50, respectively, which are estimated for $\gamma/\nu_\perp$.

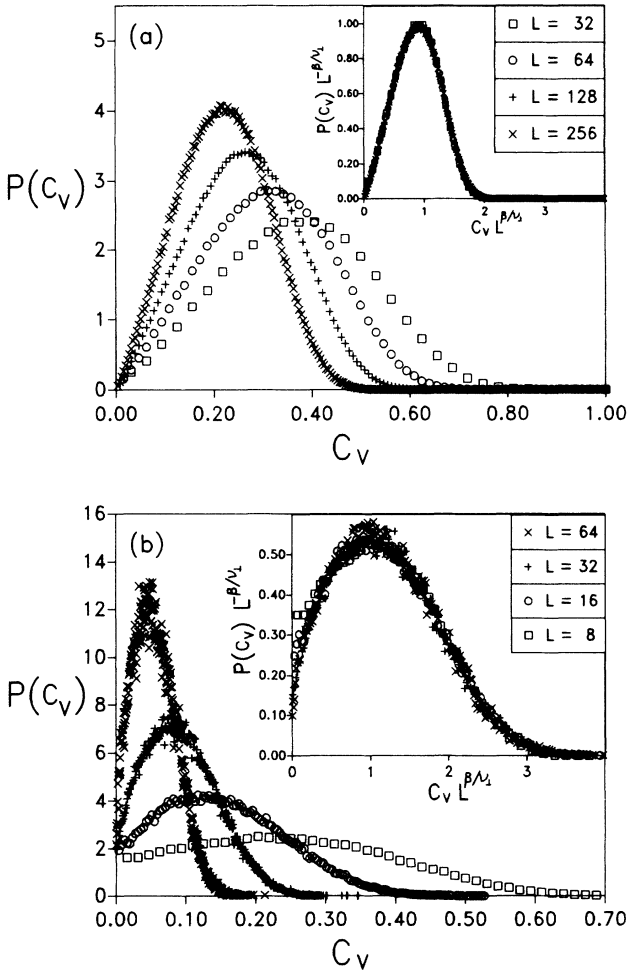

FIG. 7. The probability distribution function P_L for C_V, for (a) $p=0.2762$ in 1D and for (b) $p=0.4730$ in 2D for various system sizes L. The insets show $P_L L^{-\beta/\nu_\perp}$ vs $C_V L^{\beta/\nu_\perp}$, where $\beta/\nu_\perp$ is 0.254 in (a) and 0.741 in (b), respectively.

with $\nu_\perp \sim 0.75$, gives $\gamma \sim 0.38$. With the above results for $\nu_\perp$ and β, these results for γ are consistent with the hyperscaling relation $\gamma = \nu_\perp d - 2\beta$.

We have also studied the distribution of C_V at p_c for data sampled in the quasi-equilibrium state. In the critical region the probability distribution $P_L(C_V)$ for C_V can be expressed in terms of a scaling function $\tilde{P}$ as[15]

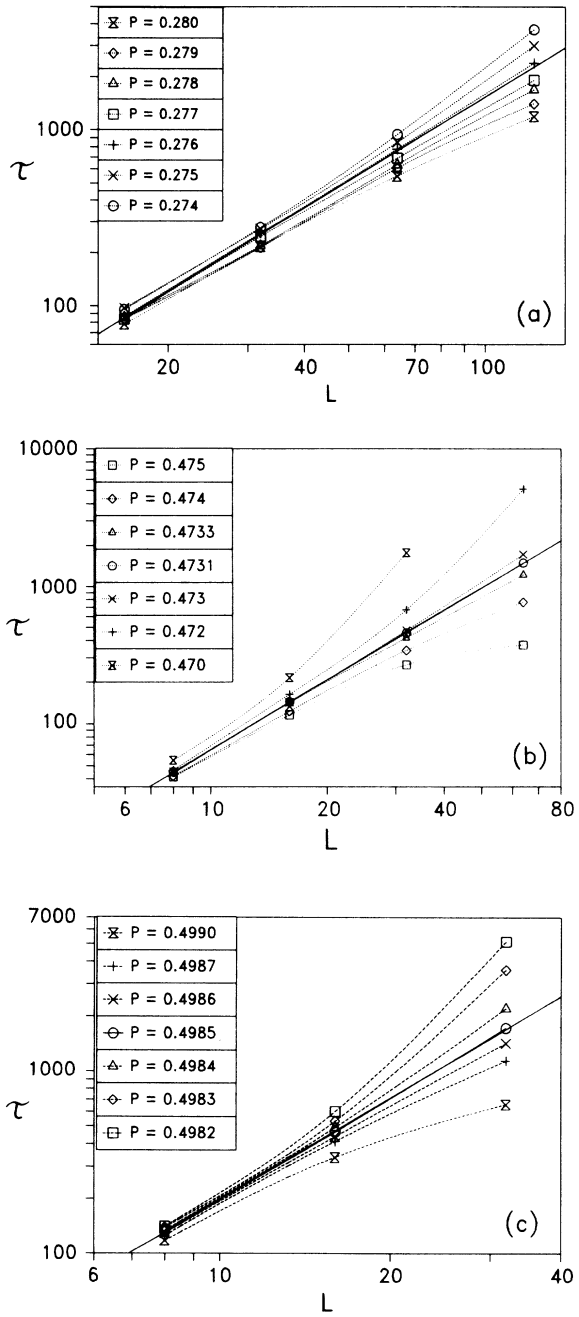

FIG. 8. $\tau(L,p)$ vs L for various values of p for (a) the 1D case, (b) the 2D case, and for (c) the 3D case on a log-log scale. The slope of the straight line which goes through the data gives an estimate of $z=\nu_\parallel/\nu_\perp$. In (a) the slope is 1.58, in (b) 1.69, and in (c) 1.85.

$$P_L(C_V)=L^{\beta/\nu_\perp}\tilde{P}(C_V L^{\beta/\nu_\perp},\xi/L)\ . \tag{16}$$

In Figs. 7(a) and 7(b) we show the distribution function $P_L(C_V)$ for C_V for $p=0.2762$ for the 1D model, and for $p=0.4730$ for the 2D model, respectively. In the inset in Figs. 7(a) and 7(b), we show $P_L(C_V)L^{-\beta/\nu_\perp}$ as a function of $C_V L^{\beta/\nu_\perp}$. By using $\beta/\nu_\perp=0.254$ for the 1D model and $\beta/\nu_\perp=0.741$ for the 2D model, as found above, the data scale well.

The above analysis of the vacancy fraction at the critical point demonstrates that, barring the covering event, there is a quasi-steady state in a finite system with strong fluctuations with time, characterized by a well-defined ensemble average.

B. Scaling results for the dynamical behavior

In Figs. 8(a)–8(c) we show $\log_{10}\tau$ versus $\log_{10}L$ for various value of p for the 1D, 2D, and 3D versions of the model, respectively. For 1D, the system size L goes from $L=16$ to $L=128$; for 2D, from $L=8$ to $L=128$; and for 3D, from $L=8$ to $L=32$. Each point is averaged over 1000 samples, except for $L=32$ in 3D where each point is averaged over 100 to 200 samples. From Eq. (15) τ should have a power-law dependence in L at p_c. Figure 8 shows that this is the case for $p=0.2762(3)$ in 1D, $p=0.4731(3)$ in 2D, and $p=0.4985(3)$ in 3D. These results are consistent with our previous estimates of p_c. In Fig. 8 the slope of the line gives $z=1.58(5)$ in 1D, $z=1.69(5)$ in 2D, and $z=1.85(10)$ in 3D. If we plot τL^{-z} [see Eq. (14)] versus $|1-p/p_c|L^{1/\nu_\perp}$ in a log-log plot (similar to the scaling of C_V), we find that all the data collapse onto a single curve for $\nu_\parallel=1.74(5)$ and $\nu_\perp=1.10(10)$ for the 1D case. In 2D we find the data points collapsing for $\nu_\parallel=1.18(10)$ and $\nu_\perp=0.70(5)$. With $\nu_\perp=0.75$ the scaling gives $\nu_\parallel\sim 1.27$. Finally in the 3D case we find $\nu_\parallel=1.05(10)$ with $\nu_\perp=0.57(5)$. With $\nu_\perp=0.60$ we find $\nu_\parallel\sim 1.1$. With the estimated error bars these results for $\nu_\perp$ are consistent with result for $\nu_\perp$ from the scaling of C_V.

We also studied the full time dependence of the mean fraction of vacancies at criticality in a different manner, which yields additional information on the dynamical behavior. The vacancy fraction $C_V(L,t,s)$ is followed in time at p_c. By averaging $C_V(L,t,s)$ over many samples one gets a quantity

$$\delta(L,t)=\langle C_V(L,t,s)\rangle_s\ , \tag{17}$$

which depends on L and time t. Note that in contrast to the procedure to obtain δ_s, the average in Eq. (17) also includes the configurations after they have reached the poisoned state. The insets in Figs. 9(a) and 9(b) show $\delta(L,t)$ versus t for $p=0.2762$ and $p=0.4731$ for the 1D and the 2D model, respectively. For $t\gg 1$ and $L\gg 1$, one can assume a scaling form

$$\delta(L,t)\sim L^{-\beta/\nu_\perp} f\delta(t/L^z)\ . \tag{18}$$

In Fig. 9 we have also plotted $\delta(L,t)L^{\beta/\nu_\perp}$ versus t/L^z. For the 1D model [Fig. 9(a)], we have used $\beta/\nu_\perp=0.254$ and $z=1.56$ as found above. In 2D [Fig. 9(b)] we have used $\beta/\nu_\perp=0.74$ and $z=1.69$. In 3D [Fig. 9(c), with $p=0.4985$] we have used $\beta/\nu_\perp=1.31$ and $z=1.85$. At p_c, the system will show critical behavior for $t<L^z$ before finite-size effects show up. Thus for $L\gg 1$ and for $t<L^z$ one can assume that $\delta(t)$ has a power-law dependence in t as

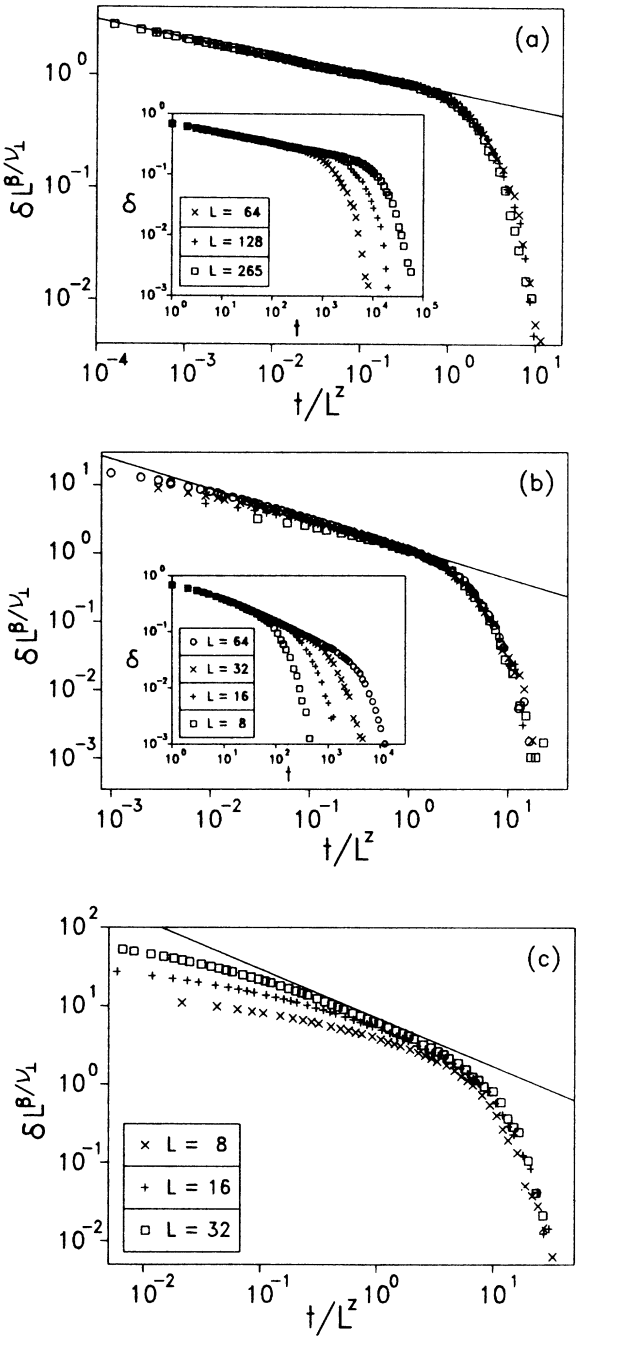

FIG. 9. Scaling of $\delta(L,t)$ as $\delta(L,t)L^{\beta/\nu_\perp}$ vs t/L^z for (a) the 1D case with $p=0.2762$, for (b) the 2D case with $p=0.4730$, and for (c) the 3D case with $p=0.4985$. In (a) $\beta/\nu_\perp=0.254$ and $z=1.58$, in (b) $\beta/\nu_\perp=0.741$ and $z=1.69$, and in (c) $\beta/\nu_\perp=1.31$ and $z=1.85$. The straight line has a slope of $\beta/(\nu_\perp z)$. The insets in (a) and (b) show $\delta(L,t)$ as a function of time t for various system sizes L.

TABLE I. Comparison of the exponents found in this work with values from directed percolation (DP) models.

Exponent	1D	2D	3D	1D DP[a]	2D DP[b]	3D DP[c]
p_c	0.2762(3)	0.4730(3)	0.4985(3)			
β	0.28(2)	0.56(5)	0.79(7)	0.280(4)	0.58	0.82
$\nu_\perp$	1.10(5)	0.75(5)	0.60(7)	1.10	0.75	0.58
$\nu_\parallel$	1.74(5)	1.27(10)	1.10(10)	1.73	1.27	1.10
γ	0.56(5)	0.38(5)				

[a]From Refs. 16 and 17.
[b]From Refs. 8 and 16.
[c]From Ref. 19.

$$\delta(t)\sim t^{-y} . \tag{19}$$

If this is to be consistent with Eq. (18) for large L one must have $y=\beta/\nu_\perp z=\beta/\nu_\parallel$. The straight lines shown in Figs. 9(a), 9(b), and 9(c), have slopes according to the ratios $-\beta/(\nu_\perp z)$ based on the values for $\beta/\nu_\perp$ and z used in the earlier scaling plots. The lines for the 1D and the 2D model show good agreement with the data. For 3D [Fig. 9(c)], the data fall on a straight line only in a small region. This is evidence that there are corrections to scaling present, and that one needs to go to larger lattices to get more accurate results in 3D.

The results for the critical exponents for the Browne-Kleban model are presented in Table I. The exponents found are practically indistinguishable from the exponents for the Reggeon field theory and directed percolation in one and two dimensions,[8,16,17] which are also shown in Table I. For three dimensions, the critical exponents for RFT and DP are based on ϵ expansion around $4+1$ dimensions,[5,18,19] the upper critical dimension for RFT and DP. In Table I we show the results from Ref. 19. These results provide strong numerical evidence that the autocatalytic reaction model is in the same universality class as RFT and DP.

V. CONCLUSIONS

We have studied a nonequilibrium reaction model transition which, at a first glance, does not seem to be anything like an equilibrium model, but actually shows very similar critical behavior. The main difference is the presence of a covered state that is a stable state for this model. The approach in this paper concentrates on scaling behavior and on dynamics. We capitalized on the finite-size scaling of the fraction of vacancies and on dynamical quantities like the covering time of a finite system. The estimates for the threshold from finite-size scaling show very good agreement with direct estimates for the threshold based on simulations of large systems. The exponents β, $\nu_\perp$, $\nu_\parallel$, and γ were obtained by independent forms of analyzing the numerical results, leading to quite accurate values. We also compared the values of the exponents to the exponents for Reggeon field theory and the directed percolation model and find very good agreement in one and two dimensions. The consistency among all the scaling relations, for both static and dynamic quantities, shows that this transition is similar to a second-order phase transition. The approach developed in this work can be generalized to deal with more complex models and reactions.

ACKNOWLEDGMENTS

We wish to thank B. Derrida, A. Hansen, and J. Houlrik for helpful discussions and comments.

*Permanent address: Department of Physics and Astronomy, Louisiana State University, Baton Rouge, Louisiana 70803.

[1]R. M. Ziff, E. Gulari, and Y. Barshad, Phys. Rev. Lett. **56**, 2553 (1986).
[2]P. Meakin and D. J. Scalapino, J. Chem. Phys. **87**, 731 (1987).
[3]R. Dickman and M. A. Burschka, Phys. Lett. **A127**, 132 (1988).
[4]V. N. Gribov, Zh. Eksp. Teor. Fiz. **53**, 654 (1967) [Sov. Phys.—JETP **26**, 414 (1968)]; H. D. I. Abarbanel, J. B. Bronzan, R. L. Sugar, and A. R. White, Phys. Rep. **21C**, 120 (1975).
[5]J. L. Cardy and R. L. Sugar, J. Phys. A **13**, L423 (1980).
[6]P. Grassberger and K. Sundermeyer, Phys. Lett. B **77**, 220 (1978).
[7]G. Grinstein, Z. W. Lai, and D. A. Browne, Phys. Rev. A **40**, 4820 (1989).
[8]R. C. Brower, M. A. Furman, and M. Moshe, Phys. Lett. B **76**, 213 (1978).
[9]D. A. Browne and P. Kleban, Phys. Rev. A **40**, 1615 (1989).
[10]T. Aukrust, D. A. Browne, and I. Webman, Europhys. Lett. **10**, 249 (1989).
[11]S. Wolfram, Physica D **10**, 1 (1986).
[12]A. De Masi, P. A. Ferrari, and J. L. Lebowitz, Phys. Rev. Lett. **55**, 1947 (1985); J. Stat. Phys. **44**, 589 (1986).
[13]R. Dickman, Phys. Rev. A **34**, 4246 (1986).
[14]A. U. Neumann and B. Derrida, J. Phys. **49**, 1647 (1988).
[15]A. Milchev, K. Binder, and D. W. Heermann, Z. Phys. B **63**, 521 (1986).
[16]W. Kinzel, Ann. Israel Phys. Soc. **5**, 425 (1983).
[17]E. Domany and W. Kinzel, Phys. Rev. Lett. **53**, 311 (1984).
[18]J. B. Bronzan and J. W. Dash, Phys. Rev. D **10**, 4208 (1974); **12**, 1850 (1975).
[19]H. K. Janssen, Z. Phys. B **42**, 151 (1981).